AJNR

Contrast-Enhanced Three-Dimensional Transcranial Color-Coded Sonography of Intracranial Stenoses

Christof Klötzsch, Alessandro Bozzato, Gero Lammers, Michael Mull and Johannes Noth

AJNR Am J Neuroradiol 2002, 23 (2) 208-212
http://www.ajnr.org/content/23/2/208

AJNR Am J Neuroradiol 23:208–212, February 2002

Contrast-Enhanced Three-Dimensional Transcranial Color-Coded Sonography of Intracranial Stenoses

Christof Klötzsch, Alessandro Bozzato, Gero Lammers, Michael Mull, and Johannes Noth

BACKGROUND AND PURPOSE: **Intracranial stenoses are associated with a considerable number of strokes each year. The clinical value of a workstation-based three-dimensional (3D) reconstruction system for transcranial color-coded sonography was evaluated in patients with intracranial stenosis or occlusion.**

METHODS: **Twenty-six patients (13 men, 13 women; mean age, 57 years ± 12 [SD]) with 36 intracranial stenoses or occlusions, as detected at two-dimensional (2D) color Doppler imaging (CDI) and digital subtraction angiography (DSA), underwent Levovist-enhanced power Doppler imaging (PDI), with subsequent 3D reconstruction. A workstation connected to a magnetic sensor capable of spatial localization of the probe was used to reconstruct 3D images of the circle of Willis from serial PDI images.**

RESULTS: **At DSA, seven (19%) stenoses were estimated to less than 50%, 24 (67%) were 50% or more, and five (14%) were occluded. DSA and 3D-PDI estimates of the degree of stenosis agreed in 33 cases (92%), with a weighted κ value of 0.86. Disagreement occurred with two subtotal basilar artery stenoses and one subtotal middle cerebral artery stenosis, which were evaluated as being complete occlusions at 3D-PDI. Interobserver agreement between two experienced 3D investigators in estimating the percentage of stenosis was high (correlation coefficient, .98).**

CONCLUSION: **3D-PDI enables the investigator to reconstruct virtually any arbitrary viewing angle. Compared with conventional CDI, 3D-PDI offers easier spatial assessment of intracranial stenoses, and its findings are sufficiently correlated with angiographic findings. Because different investigators can postprocess the same 3D data, improving reproducibility and reducing investigator dependency in transcranial color-coded sonography may be possible.**

Stenoses of the intracranial arteries are less common than atherosclerosis of the extracranial vessels, but they are associated with a considerable number of strokes each year (1–3). Several studies have addressed the detection of intracranial stenoses with transcranial Doppler sonography (TCD) (4–8) or transcranial color-coded sonography (9–14). The value of transcranial color Doppler imaging (CDI) as a tool in the diagnosis of vascular alterations is unquestioned. Advantages lie in the ability to obtain angle-corrected flow velocity measurements (15) and to precisely locate the intracranial stenosis (9). However, demonstration of the spatial dimensions of the stenosis with CDI is possible in only a minority of patients (11). The purpose of this study was to determine the preliminary clinical value of a new workstation-based three-dimensional (3D) reconstruction system (16) for transcranial sonography in patients with intracranial stenoses or occlusions.

Received December 4, 2000; accepted after revision September 19, 2001.

From the Departments of Neurology (C.K., A.B., G.L., J.N.) and Neuroradiology (M.M.), Universitätsklinikum der Rheinisch-Westfälischen Technischen Hochschule Aachen, Germany.

This study was supported by a grant START 28/97 S from the University of Aachen.

Address reprint requests to Christof Klötzsch, MD, Department of Neurology, RWTH Aachen, 52057 Aachen, Germany.

Methods

Selection of Patients

The study included patients with cerebral ischemia in whom at least one intracranial stenosis or occlusion was detected during nonenhanced CDI examination (Acuson XP128/10, 2-MHz phased-array probe; Mountain View, CA). Twenty-six consecutive patients with intracranial stenosis or occlusion or both (13 men, 13 women; mean age 57 years ± 12 SD) fulfilled the criteria. All patients provided informed consent.

The circle of Willis and the foramen magnum were insonated through both temporal bone windows. To estimate the of degree of stenosis, we used a Doppler sonographic classification system, which Baumgartner et al (11) validated with

intraarterial digital subtraction angiography (DSA). Stenoses were classified as less than 50% luminal narrowing and 50% or more luminal narrowing, according to the individual peak flow velocities in the intracranial arteries. The minimal peak systolic velocity cutoff values for stenosis of less than 50% and those of 50% or more, respectively, were the following: anterior cerebral artery (ACA), 120 and 155 cm/s; middle cerebral artery (MCA), 155 and 220 cm/s; posterior cerebral artery (PCA), 100 and 145 cm/s; basilar artery (BA), 100 and 140 cm/s; and vertebral artery (VA), 100 and 145 cm/s. Furthermore, we semiquantitatively estimated the extent of low- and high-intensity signals in the Doppler spectrum of the stenotic vessel segment. Angle correction was used only if CDI findings suggested the presence of a straight vessel segment with a length of least 20 mm (17). Intracranial occlusion was diagnosed when the Doppler signal in the corresponding cerebral artery was lacking and when the other ipsilateral basal cerebral arteries were identified. In all pateints, the extracranial cerebral arteries were examined by using the same duplex machine with a 5.0- or 7.0-MHz linear probe.

3D Sonography

During contrast-enhanced 3D power Doppler imaging (PDI), the investigator (C.K.) was aware that at least one intracranial stenosis or occlusion or both was found on the previous CDI scan. He was, however, blinded to the precise location and degree of the stenosis. We did not perform nonenhanced 3D-PDI in the present study, because a previously published study (18) of 3D-PDI in intracranial aneurysms revealed frequent vessel discontinuity and insufficient differentiation regarding background signals.

Contrast enhancement was achieved by means of an intravenous injection of a transpulmonary stable agent. This consisted of galactose microparticles and a small amount of palmitic acid–stabilizing air microbubbles (Levovist; Schering, Germany). Levovist is approved in Germany for contrast material–enhanced vascular sonography. To reach a stable contrast enhancement of 15–20 dB for 8–10 min without blooming artifacts, the contrast agent was continuously administered (2.5 g; 300 mg/mL; rate, 1 mL/min) by using a perfusor (P4000 IVAC, Basingstoke, England).

For a precise demonstration of vessel dimensions during contrast-enhanced 3D-PDI, changing some parameters of the duplex machine was important. The color persistence was markedly reduced, and the color Doppler gain was reduced to prevent blooming artifacts. These reductions usually resulted in a lack of vessel continuity in the two-dimensional (2D) mode, but the summation effects of 150–200 consecutive images allowed sufficient demonstration of the vessel lumen. All contrast-enhanced studies were performed by using fundamental frequencies. The output power level used in this study was less than 100 mW/cm^2, which is approved by the Food and Drug Adminsitration and the European administrations for transcranial sonography.

The free-hand system (3D Echotech; Hallberginoos, Germany) used in this study is adaptable to every commercially available color-coded duplex system. The 3D system consisted of an electric magnet, which induces a low magnetic field near the head of the patient. The composite magnetic field was generated from an array of three coils, which are arranged at 90° angles to each other to yield a 3D orientation. A magnetic position sensor was attached to the ultrasound probe and transmitted the spatial orientation (x, y, z axes) of the probe to a workstation (two 400-MHz Pentium processors, 512 MB random-access memory), which also received the corresponding 2D images from the video port of the duplex machine. This approach allowed the operator to move the transducer without constraint. To acquire a 3D data block in the circle of Willis, the transducer was tilted around an axis that was perpendicular to the central axis of the transducer (fanlike rotation) and slowly moved across the temporal bone window or the occipital approach. In 30–40 s, 150 2D images and the spatial information were stored on the hard disk of the workstation. During offline analysis, a reconstruction algorithm was used to extract the color-coded information from the 3D data set. The Windows NT 4.0–based software provided photorealistic surface rendering of the vessels being examined. An experienced sonographer who was familiar with the equipment was able to produce an animated 3D image of the circle of Willis in 5 min.

TABLE 1: Classification of 36 intracranial stenoses and occlusions with CDI and DSA

	CDI Finding			
DSA Finding	Normal	Stenosis <50%	Stenosis ≥50%	Occlusion
Normal	0	0	0	0
Stenosis <50%	2	2	3	0
Stenosis ≥50%	6	5	13	0
Occlusion	0	0	0	5

Note.—The weighted κ value was 0.376.

Angiography

DSA was performed after 2D CDI and 3D-PDI. In all 26 patients, the clinical decision to perform DSA was made within 4 days of the initial sonographic examination. Four-vessel angiography was performed with a femoral approach by using a Siemens Neurostar unit. The volume of contrast medium (Ultravist 300; Schering) injected was 5–8 mL. Standard anteroposterior and lateral views (1024 × 1024 matrix) were routinely obtained. To evaluate the stenosis with DSA and 3D-PDI, the residual lumen was compared with the normal diameter of the distal part of the vessel. Stenoses were classified as than 50% or 50% or more.

Statistical Analysis

Semiquantitative estimates of the degree of stenosis with DSA, CDI, and 3D-PDI were compared by using the weighted κ coefficient. Linear regression analysis was used to investigate interobserver variability with 3D-PDI in the evaluation of the diameter of the stenosis.

Results

Angiography revealed 15 intracranial stenoses or occlusions or both in the MCA, whereas eight stenoses were present in the intracranial segment of the internal carotid artery (ICA). Four of these stenoses were in the ICA cisternal segment (IC_1A), while the remaining four stenoses were located in the carotid siphon. Other stenoses and/or occlusions were observed in the PCA (n = 6), ACA (n = 1), distal BA (n = 3), and distal segment of the VA (V_4A) (n = 3).

Correlation of Nonenhanced CDI Findings with DSA Findings

Twenty-three stenoses and five occlusions (78%) were initially detected at CDI (Table 1). Three stenoses in the MCA main stem (M_1CA) were estimated to be 50% or more, but DSA demostrated a stenosis of less than 50%. Five stenoses (two in the MC_1A, one in the IC_2A, one in the MCA insular branches [M_2CA], and one in the PCA precommunicating seg-

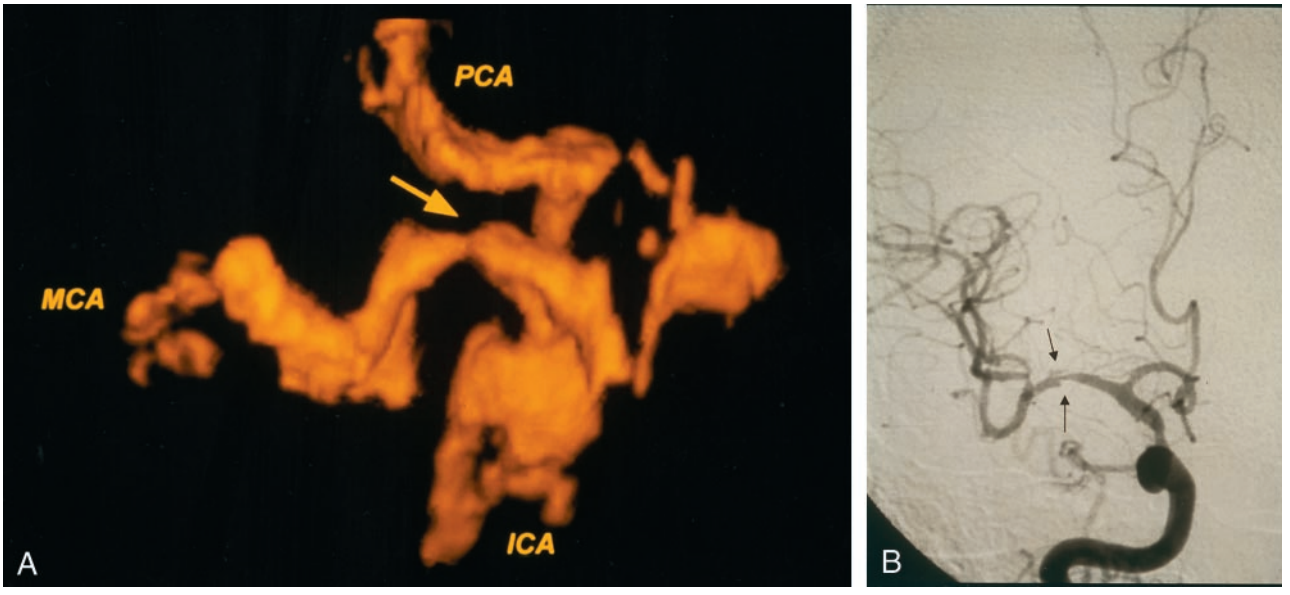

FIG 1. Anteroposterior images of an intracranial stenosis.
A, 3D-PDI image shows the circle of Willis with a severe stenosis (*arrow*) in the MCA.
B, Angiogram confirms a severe stenosis (*arrows*) in the MCA stem.

ment [P_1CA]) were estimated to be less than 50% at CDI, but DSA revealed stenoses of 50% or more. Two stenoses of less than 50% and six of 50% or more were overlooked with CDI. These stenoses were located in the M_1CA (n = 1), the PCA postcommunicating segment (P_2CA) (n = 4), the ICA cavernosal segment (IC_4A) (n = 1), and the distal part of the BA (n = 2). In the case of the M_1CA stenosis, angiography revealed a large branch proximal to the subtotal stenosis, which was regarded as the MCA stem. Additional factors that influenced the correct estimation of the intracranial stenoses were an insufficient acoustic bone window (n = 4) and a reduction in flow velocity due to a stenosis of 70% or more that was proximal to the intracranial stenosis (n = 6). On the basis of the classification used (less than 50%, 50% or more), the weighted κ value for the agreement between DSA and CDI findings in the estimation of the degree of stenosis was 0.376.

Correlation of Contrast-enhanced 3D-PDI Findings with DSA Findings

The maximum interval between 3D-PDI and DSA was 2 days. At DSA seven (19%) stenoses were estimated to be less than 50%, 24 (67%) were narrowed by 50% or more, and the remaining five (14%) vessels were occluded. In 33 stenoses (92%), we observed complete agreement between the estimations of the degree of stenosis with DSA and 3D-PDI (Fig 1, Table 2). Disagreement was observed in two subtotal distal BA stenoses and one subtotal M_1CA stenosis, which were diagnosed as occlusions at 3D-PDI. The weighted κ value in the estimation of the degree of stenosis with DSA and 3D-PDI was 0.86. Two experienced 3D-PDI investigators (C.K., A.B.) independently evaluted all datasets. The interobserver correlation (Fig 2) in estimating the percentage of stenosis by using the two datasets in each patient was high (r = .98).

TABLE 2: Classification of 36 intracranial stenoses and occlusions with 3D PDI and DSA

	3D PDI Finding			
DSA Finding	Normal	Stenosis <50%	Stenosis ≥50%	Occlusion
Normal	0	0	0	0
Stenosis <50%	0	7	0	0
Stenosis ≥50%	0	0	21	3
Occlusion	0	0	0	5

Note.—The weighted κ value was 0.86.

Discussion

The findings of several studies have shown that CDI is superior to TCD in the detection of acute MCA occlusion (19–22). However, commonly accepted Doppler sonographic criteria for the classification of intracranial stenoses are not available. Baumgartner et al (11) recently proposed an angiographically validated classification system in which stenoses of less than 50% and those of 50% or more are grouped by using cutoff values for the peak flow velocities in each vessel; this system was used in our examinations.

The correlation of our CDI and DSA data resulted in agreement that was remarkably lower than that of previously published studies (9, 11). Nonenhanced CDI failed to depict eight (22%) stenoses, but these stenoses often were difficult to insonate. Stenoses in the P_2CA had to be insonated with an unfavorable angle of 90° near the brain stem. The same problem occurred in two subtotal stenoses in the distal BA.

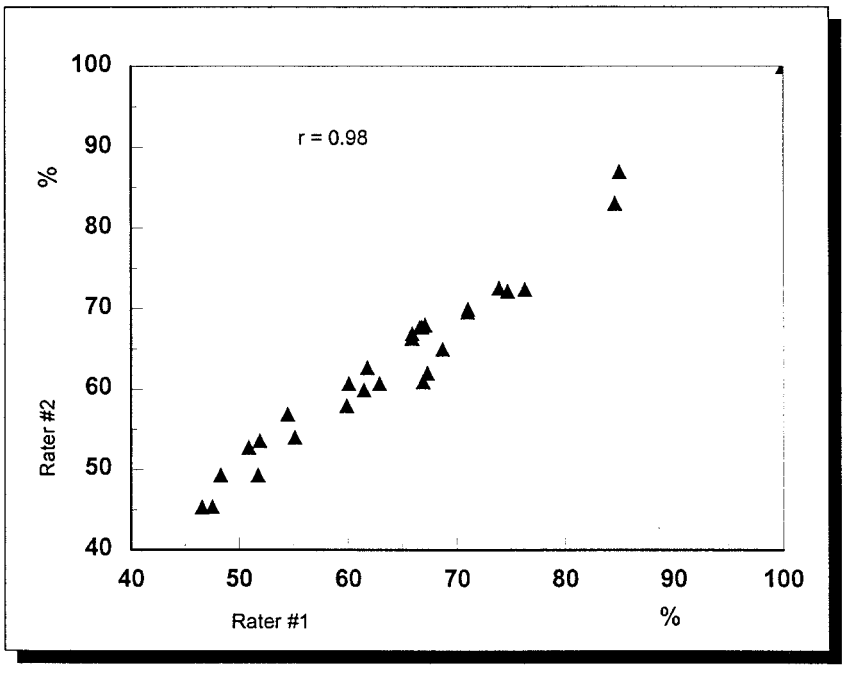

FIG 2. Plot shows the interobserver correlation between the two experienced 3D-PDI investigators in the estimation of the percentage of stenosis.

One stenosis of the IC_4A could not be reliably evaluated with CDI because of its proximity to the skull. In one M_1CA stenosis, angiography revealed a large branch proximal to the subtotal stenosis; therefore CDI results caused misdiagnosis in an M_1CA. Partial recanalization is the most likely cause of the finding of less stenosis at DSA, compared with CDI, in the three patients with stenoses of less than 50%. After DSA, these three patients underwent a second CDI examination, and this time, the sonographic and angiographic degrees of stenosis were identical.

Since the acoustic bone windows were insufficient in four patients, the detection rate with CDI could have been substantially better if contrast enhancement had been used (10, 12, 21, 22). However, the fact that the detected flow velocities would have been higher (23) and that no classification of intracranial stenoses under these conditions is yet available must be taken into account. Because of the reduction in the poststenotic flow velocity, the hemodynamic assessment of intracranial stenoses may be impaired if stenoses of 70% or more occur proximal to the intracranial stenosis. In the present study, this was observed in six patients.

If different insonation angles are used at CDI, differentiation of MCA trunk stenosis from intracranial ICA branch or MCA branch stenosis usually is possible (9). However, CDI cannot offer exact 2D information about the stenosis (11), because the increase in intrastenotic velocity may persist for 10–15 mm and surpass the anatomic extent of the narrowing. 3D-PDI is a new noninvasive method for the investigation of intracranial vessel disease (16). Compared with CDI, 3D-PDI permits easier differentiation between artifacts and real changes of the vessel anatomy, and its results are sufficiently correlated with those of the criterion standard, DSA (18). PDI is better suited for 3D reconstruction than is CDI, because it is more sensitive in depicting low flow near the vessel wall, and its images are less degraded by noise and clutter (14). The additional use of an echo contrast agent facilitates the 3D reconstruction of small vascular alterations.

The present DSA and 3D-PDI findings completely agreed in 92% of the cases, but they revealed limitations of 3D-PDI in the differentiation of subtotal stenosis from occlusion. The main reason for this is the inability of 3D-PDI to depict an extremely reduced residual lumen in intracranial stenoses. However, in contrast to CDI, 3D reconstruction of intracranial stenosis is not affected by proximal or extracranial stenosis of 70% or more. Compared with CDI and angiography, 3D-PDI enables the investigator to reconstruct virtually any arbitrary viewing an gle. Because different invesigators can postprocess the same 3D data, improving reproducibility and reducing investigator dependency in transcranial color-coded sonography may be possible. This possibility is higlighted in the presented study by the high correlation coefficient of .98 between the two independent 3D-PDI investigators in the estimation of the degree of stenosis with the use of different datasets in each patient.

3D-PDI provides lower resolution than that of CT angiography (CTA) or MR angiography (MRA), but repeat examinations easily can be performed in critically ill patients in stroke or intensive care units. At CTA or MRA, patients with stroke often need sedation or even intubation and ventilation to ensure that they remain in a resting position during the examination. Compared with the iodic contrast agents used for CTA, the only contraindications for the echo contrast agent Levovist are galactosemia (which is rare), severe heart insufficiency (New York Heart

Association grades III or IV), and severe obstructive pulmonary disease.

From MRA studies, it is well known that, in severe stenoses, an occlusion can be diagnosed if turbulences or a poststenotic decrease in flow velocity causes signal loss (24). Another study (25) revealed an agreement of 88% between MRA results and DSA results in all intracranial stenoses, but in intracranial VA stenoses, the agreement was only 65%. With the use of CTA, data acquisition for intracranial vessel image reconstruction needs only 1 minute, but Lehmann et al (26) observed a tendency to underestimate stenoses at CTA. Technical limitations of CTA are the superposition of venous vessels or the skull (26, 27) and the time-consuming postprocessing of the 3D datasets. On the other hand, 3D reconstructions of the PDI parenchymal data easily can be subtracted from vascular data with one mouse click. The computer-based 3D reconstruction needs less than a minute, because the vascular information is only 30–40 MB.

Conclusion

The present study has several limitations: Only preliminary conclusions are possible, because we did not include patients without intracranial stenoses, and the contrast agent was used only at 3D-PDI and not in CDI. We used nonenhanced CDI because, at the time, this was the standard method for transcranial sonographic imaging. However, to our knowledge, the present study is the first in which the data obtained with 3D-PDI and DSA are compared in a considerable number of patients with intracranial stenoses. The major aim of the study was to show what is currently possible in the demonstration of intracranial stenoses at 3D sonography. 3D-PDI does not replace hemodynamic assessment of intracranial stenoses with conventional CDI, but the 3D reconstruction of vascular alterations may be an interesting additional tool, especially for follow-up investigations. Furthermore, 3D-PDI can be a help in the sonographic assessment of intracranial vessel disease for those who are not familiar with the technique of transcranial color-coded sonography.

Acknowledgments

For assistance in preparing the manuscript, we thank Stuart Fellows, Department of Neurology, RWTH Aachen, Germany. The authors thanks Professor Klaus Willmes von Hinckeldey, Department of Neuropsychology, RWTH Aachen, Germany, for assistance in the statistical evaluation of the presented data.

References

1. Chimowitz MI, Kokkinos J, Strong J, et al. **The warfarin-aspirin symptomatic intracranial disease study.** *Neurology* 1995;45:1488–1493
2. Marzewski DJ, Furlan AJ, St Louis P, Little JR, Modic MT, Williams G. **Intracranial internal carotid artery stenosis: longterm prognosis.** *Stroke* 1982;13:821–824
3. Wechsler LR, Kistler JP, Davis KR, Kaminski MJ. **The prognosis of carotid siphon stenosis.** *Stroke* 1986;17:714–718
4. Ley-Pozo J, Ringelstein EB. **Noninvasive detection of occlusive disease of the carotid siphon and middle cerebral artery.** *Ann Neurol* 1990;28:640–647
5. Mattle H, Grolimund P, Huber P, Sturzenegger M, Zurbrügg HR. **Transcranial Doppler sonographic findings in middle cerebral artery disease.** *Arch Neurol* 1988;45:289–295
6. Rorick MB, Nichols FT, Adams RJ. **Transcranial Doppler correlation with angiography in detection of intracranial stenosis.** *Stroke* 1994;25:1931–1934
7. Schwarze JJ, Babikian V, DeWitt LD, et al. **Longitudinal monitoring of intracranial arterial stenoses with transcranial Doppler ultrasonography.** *J Neuroimaging* 1994;4:182–187
8. Zanette EM, Fieschi C, Bozzao L, et al. **Comparison of cerebral angiography and transcranial Doppler sonography in acute stroke.** *Stroke* 1989;20:899–903
9. Klötzsch C, Popescu O, Sliwka U, Mull M, Noth J. **Detection of stenoses in the anterior circulation using frequency based transcranial color-coded sonography.** *Ultrasound Med Biol* 2000;26:579–584
10. Goertler M, Kross R, Bäumer M, et al. **Diagnostic impact and prognostic relevance of early contrast-enhanced transcranial color-coded duplexsonography in acute stroke.** *Stroke* 1998;29:955–962
11. Baumgartner RW, Mattle HP, Schroth G. **Assessment of >50% and <50% intracranial stenoses by transcranial color-coded duplex sonography.** *Stroke* 1999;30:87–92
12. Nabavi DG, Droste DW, Kemeny V, Schulte-Altedorneburg G, Weber S, Ringelstein RW. **Potential and limitations of echocontrast-enhanced ultrasonography in acute stroke patients.** *Stroke* 1998;29:949–954
13. Kimura K, Yasaka M, Wada K, Minematsu K, Yamaguchi T, Otsubo R. **Diagnosis of middle cerebral artery stenosis by transcranial color-coded real-time sonography.** *Am J Neuroradiol* 1998;19:1893–1896
14. Griewing B, Schminke U, Motsch L, Brassel F, Kessler C. **Transcranial duplex sonography of middle cerebral artery stenosis: a comparison of colour-coding techniques–frequency or power-based Doppler and contrast enhancement.** *Neuroradiology* 1998;40:490–495
15. Baumgartner RW, Mathis J, Sturzenegger M, Mattle HP. **A validation study on the intraobserver reproducibility of transcranial color-coded duplex sonography velocity measurements.** *Ultrasound Med Biol* 1994;20:233–237
16. Delcker A, Turowski B. **Diagnostic value of three-dimensional transcranial contrast duplex sonography.** *J Neuroimaging* 1997;7:139–144
17. Giller CA. **Is angle correction correct?** *J Neuroimaging* 1994;4:51–52
18. Klötzsch C, Bozzato A, Lammers G, Mull M, Lennartz B, Noth J. **Three-dimensional transcranial color-coded duplexsonography of cerebral aneurysms.** *Stroke* 1999;30:2285–2290
19. Martin PJ, Pye IF, Abbott RJ, Naylor AR. **Color-coded ultrasound diagnosis of vascular occlusion in acute ischemic stroke.** *J Neuroimaging* 1995;5:152–156
20. Kenton AR, Martin PJ, Abbott RJ, Moody AR. **Comparison of transcranial color-coded sonography and magnetic resonance angiography in acute stroke.** *Stroke* 1997;28:1601–1606
21. Gerriets T, Seidel G, Fiss I, Modrau B, Kaps M. **Contrast-enhanced transcranial color-coded duplex sonography: efficiency and validity.** *Neurology* 1999;52:1133–1137
22. Postert M, Braun B, Federlein J, Przuntek H, Köster O, Büttner T. **Diagnosis and monitoring of middle cerebral artery occlusion with contrast enhanced transcranial color-coded real-time sonography in patients with inadequate acoustic bone windows.** *Ultrasound Med Biol* 1998;24:333–340
23. Goldberg BB, Liu JB, Forsberg F. **Ultrasound contrast agents: a review.** *Ultrasound Med Biol* 1994;20:319–333
24. Wilcock DJ, Jaspan T, Worthington BS. **Problems and pitfalls of 3-D TOF magnetic resonance angiography.** *Clin Radiol* 1995;50:526–532
25. Dagirmanjian A, Ross JS, Obuchowski N, et al. **High resolution magnetization transfer saturation, flip angle, time-of-flight MRA in the detection of intracranial vascular stenoses.** *J Comput Assist Tomogr* 1995;19:700–706
26. Lehmann KJ, Neff KW, Ries S, Sommer A, Steinke W, Georgi M. **Spiral-CT angiography in stenoses of the middle cerebral artery.** *Radiologe* 1996;36:845–849
27. Wilms G, Guffens M, Gryspeerdt S et al. **Spiral CT of intracranial aneurysms: correlation with digital subtraction and magnetic resonance angiography.** *Neuroradiology* 1996;38:20–25